Conversion in the Solid State of the Yellow to the Red Form of 2-(4′-Methoxyphenyl)-1,4-benzoquinone. X-Ray Crystal Structures and Anisotropy of the Rearrangement[1,2]

Gautam R. Desiraju, Iain C. Paul,* and David Y. Curtin*

Contribution from the Department of Chemistry and the Materials Research Laboratory, University of Illinois, Urbana, Illinois 61801. *Received June 1, 1976*

Abstract: The thermal rearrangement in the solid state of the yellow (**1a**) to the red (**1b**) crystalline form of 2-(4′-methoxyphenyl)-1,4-benzoquinone has been studied. Single crystals rearrange by a process which begins at a limited number of nucleation sites in the crystal and spreads by migration of well-defined fronts. X-ray crystal structures of **1a** and **1b** have been determined. The yellow crystals of **1a** are orthorhombic, $a = 6.719$ (2), $b = 7.168$ (3), $c = 44.206$ (18) Å; the space group is *Pbca*, and the structure has been refined to an R factor of 0.043 on 1473 nonzero reflections. The red form **1b** is orthorhombic, $a = 12.783$ (2), $b = 6.969$ (2), $c = 23.369$ (5) Å; the space group is *Pbca*, and the structure has been refined to an R factor of 0.052 on 1530 nonzero reflections. The structures are each composed of racemic pairs of molecules, a particular molecule being chiral by virtue of the nonplanar arrangement of the two six-membered rings. The yellow and the red constituent molecules are related to each other as diastereoisomers. The difference in the color is accounted for by the stacking of the molecules in the yellow form with overlap between adjacent quinone rings, whereas in the red form there is π complexing between quinone and anisyl rings. As might have been anticipated, this complexing leads to some alteration of bond distances in the red form.

Organic compounds in the solid state can undergo chemical changes which, both in their structural alterations and in their mechanisms, are unparalleled in solution.[3-5] The present investigation of a solid state process was prompted by the observation[6-8] that 2-(4′-methoxyphenyl)-1,4-benzoquinone (*p*-anisylquinone) (**1**) crystallizes as both a yellow (**1a**) and

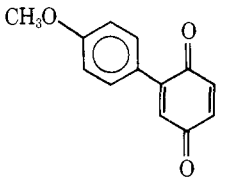

1

a red (**1b**) crystalline solid and that the yellow solid undergoes a thermal reaction to give the red form. In this paper we report the discovery that the reaction of single crystals of **1a** is highly anisotropic and may originate at a strictly limited number of nucleation sites. X-ray crystal structure determinations of **1a** and **1b** have been carried out, and the relationship between the observed anisotropy and the change in structure is discussed.

Experimental Section

Melting points were measured on a Mettler FP21 hot stage connected to a Mettler FP2 control unit with a built-in Platinum Resistance Thermometer and are corrected. All photographs were taken using a Mettler FP21 hot stage on a Bausch and Lomb polarizing microscope equipped with a Beseler Topcon Super D camera. Kodak high-speed Ektachrome film (tungsten-3200 K) was used. The differential thermal analysis studies were done using a du Pont 900 instrument.

2-(4′-Methoxyphenyl)-1,4-benzoquinone (1) was made in nearly quantitative yield by the method of Brassard and L'Écuyer.[9] Recrystallization of the crude material from 1:1 EtOH–water gave a solid, mp 118 °C. Recrystallization by cooling a hot solution of 0.5 g of material in ca. 5 ml of 1:1 benzene–hexane yielded yellow plates of **1a** with (001) as the prominent face: interfacial angles obsd (calcd), (001): (010) 89° (90.0°), (001): (110) 90° (90.0°), (110): ($1\bar{1}0$) 132.5° (133.1°), (110): (010) 95° (93.7°). Slow evaporation of dilute solutions in 1:1 benzene–hexane or petroleum ether gave red crystals of **1b**: mp 121.1–122.1 °C; IR (KBr) 1655, 1607, 1588 and 1252 cm^{-1}; NMR (Me_2SO-d_6): δ 6.8–7.6 (m, 7 H), 3.8 (s, 3 H). The IR and NMR spectra of the two forms were similar.

2-(2′-Methoxyphenyl)-1,4-benzoquinone was prepared from *o*-anisidine.[9] It was necessary to extract the reaction mixture with hot petroleum ether (bp 90–110 °C) to obtain an oil that was induced to crystallize to give a red solid, in 30% yield: mp (after turning yellow) 59–63 °C; IR (KBr) 1658, 1600, 1288, and 1252 cm^{-1}; NMR (acetone-d_6) δ 6.8–7.5 (m, 7 H), 3.75 (s, 3 H).

The red solid sublimes with difficulty to give a yellow solid whose IR and NMR spectra are identical with those of the red. It may be noted that while the red form **1b** of the *p*-anisylquinone **1** is more stable than the form **1a**, it is the yellow form of the *o*-anisylquinone that is the more stable.

Studies on the Transformation of 1a to 1b in the Solid State. A Mettler hot stage was placed on a Bausch and Lomb polarizing microscope equipped with a Bessler Topcon camera. A crystal of **1a** of dimensions of 0.1 to 1.3 mm was placed on a microscope slide and fitted in the hot stage. The crystal was heated rapidly till it reached a temperature of 60 °C and was then allowed to heat up to about 85 °C in half an hour. The rearrangement was initiated at a temperature of 60–90 °C and was over in less than a minute when reaction was induced at the higher temperatures. At 60 °C it required 4 h. The crystal was photographed as viewed through transmitted light during the transformation (Figure 1).

Differential Thermal Analysis Studies. Three runs of ground **1a** and two runs of ground **1b** were made. The small exotherm corresponding to the rearrangement of **1a** to **1b** had an extrapolated onset of 66° (uncorrected) and was followed by a melting endotherm with extrapolated onset of 124°.[10,11]

X-Ray Structure Determination of the Yellow Form of *p*-Anisylquinone (1a). Crystal Data. $C_{13}H_{10}O_3$, $M = 214.22$, orthorhombic, $a = 6.719$ (2), $b = 7.168$ (3), $c = 44.206$ (18) Å, $V = 2129 \times 10^{-24}$ cm^3, F (000) = 896, $\mu = 8.12$ cm^{-1} (Cu K_α), $\rho_{calcd} = 1.32$, $Z = 8$, systematic absences; $0kl$, $k = 2n + 1$; $h0l$, $l = 2n + 1$; $hk0$, $h = 2n + 1$, lead unambiguously to the space group *Pbca* (no. 61)[12] (Cu K_α, $\lambda = 1.5418$ Å).

Collection and Reduction of Diffractometer Data. Intensity data were collected on a crystal (0.4 × 0.4 × 0.2 mm) obtained by recrystallization from 1:1 benzene hexane. The general procedures have been described previously.[13] All unique reflections within the 2θ range of 2–130° were measured using a moving-crystal moving-counter technique at a scan rate of 1° min^{-1}. There was no evidence for crystal deterioration. Of the 2188 unique reflections, 1473 (67%) were considered observed at the 3σ level. The structure was solved by direct-methods using the FAME-MAGIC-LINK-SYMPL series of programs.[14] Full-matrix, least-squares refinement, varying the positional and anisotropic thermal parameters for the nonhydrogen atoms and the positional and isotropic thermal parameters for the hydrogen atoms, gave final values of R and R_w[15] of 0.043 and 0.049, respectively. There was no evidence from a final difference map for significant electron density not included in the model. The final values of the atomic coordinates and thermal parameters are given in Tables I and II. The

Table I. Atomic Coordinates in Fractional Crystal Coordinates for **1a**[a,b]

Atom	x	y	z
C(1)	0.6133 (3)	0.3784 (3)	0.453 71 (4)
C(2)	0.4145 (3)	0.3535 (3)	0.466 64 (4)
C(3)	0.2546 (3)	0.3870 (3)	0.450 14 (4)
C(4)	0.2682 (3)	0.4522 (3)	0.418 65 (4)
C(5)	0.4704 (2)	0.4674 (2)	0.404 52 (4)
C(6)	0.6285 (3)	0.4381 (3)	0.422 12 (4)
C(7)	0.4842 (2)	0.5207 (2)	0.372 33 (4)
C(8)	0.6319 (3)	0.6411 (3)	0.362 49 (4)
C(9)	0.6461 (3)	0.6970 (3)	0.332 57 (4)
C(10)	0.5115 (3)	0.6289 (2)	0.311 74 (4)
C(11)	0.3675 (3)	0.5029 (3)	0.320 85 (4)
C(12)	0.3523 (3)	0.4508 (3)	0.350 58 (4)
C(13)	0.6434 (5)	0.8159 (5)	0.271 96 (6)
O(1)	0.7623 (3)	0.3475 (3)	0.468 78 (3)
O(2)	0.1190 (2)	0.4997 (2)	0.405 04 (3)
O(3)	0.5092 (2)	0.6758 (2)	0.281 74(3)
H(2)	0.413 (3)	0.315 (3)	0.487 8 (5)
H(3)	0.119 (3)	0.383 (3)	0.458 0 (5)
H(6)	0.762 (3)	0.445 (3)	0.414 1 (5)
H(8)	0.724 (3)	0.692 (3)	0.377 2 (4)
H(9)	0.744 (4)	0.789 (3)	0.327 0 (4)
H(11)	0.283 (3)	0.454 (3)	0.305 8 (5)
H(12)	0.248 (3)	0.361 (3)	0.356 6 (4)
H(13A)	0.781 (4)	0.790 (4)	0.277 4 (6)
H(13B)	0.618 (5)	0.938 (5)	0.283 4 (8)
H(13C)	0.617 (4)	0.835 (4)	0.250 7 (6)

[a] Estimated standard deviations are given in parentheses. [b] For labeling of atoms see Figure 4.

observed and calculated structure factors are available as supplementary material (see paragraph at end of text regarding supplementary material).

X-Ray Structure Determination of the Red Form of Anisylquinone 1b. Crystal Data. $C_{13}H_{10}O_3$, M = 214.22, orthorhombic, a = 12.783 (2), b = 6.969 (2), c = 23.369 (5) Å, $V = 2082 \times 10^{-24}$ cm^3, F (000) = 896, μ = 8.12 cm^{-1} (Cu K$_\alpha$), ρ_{calcd} = 1.41, Z = 8, systematic absences: $0kl$, $k = 2n + 1$; $h0l$, $l = 2n + 1$; $hk0$, $h = 2n + 1$, lead unambiguously to the space group *Pbca* (no. 61) (λ(Cu K$_\alpha$) = 1.5418 Å).

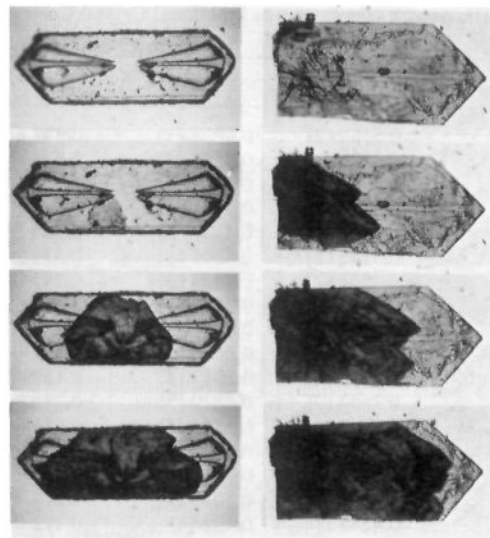

Figure 1. Thermal rearrangement of **1a** to **1b.** Left series: A crystal heated at about 87 °C. Photographs were taken at intervals of a few seconds. Note that although there were imperfections in the crystal before reaction began (top photograph) they have had no discernible effect on the progress of the reaction. Right series: Reaction of a second crystal at 87 °C showing more clearly the preference for frontal development in the [110] and [1$\bar{1}$0] directions.

Collection and Reduction of Diffractometer Data. Intensity data were collected on a crystal of **1b** (0.6 × 0.5 × 0.2 mm) grown by recrystallization from petroleum ether (bp 30–60 °C). General procedures for data collection have been described previously.[13] All unique

Table II. Thermal Parameters for **1a**[a]

Atom	B_θ or β_{11}	β_{22}	β_{33}	β_{12}	β_{13}	β_{23}
C(1)	0.0230 (5)	0.0254 (5)	0.000 384 (10)	0.0013 (4)	0.000 01 (6)	0.000 38 (6)
C(2)	0.0286 (6)	0.0246 (5)	0.000 371 (10)	−0.0001 (4)	0.000 68 (7)	0.000 58 (6)
C(3)	0.0228 (5)	0.0234 (5)	0.000 487 (11)	−0.0011 (4)	0.001 11 (7)	0.000 20 (6)
C(4)	0.0177 (4)	0.0188 (4)	0.000 429 (10)	−0.0010 (4)	0.000 38 (6)	−0.000 12 (5)
C(5)	0.0154 (4)	0.0141 (3)	0.000 373 (9)	−0.0010 (3)	0.000 27 (5)	−0.000 04 (4)
C(6)	0.0170 (5)	0.0219 (4)	0.000 377 (10)	−0.0001 (4)	0.000 16 (6)	0.000 21 (5)
C(7)	0.0147 (4)	0.0143 (3)	0.000 359 (9)	−0.0001 (3)	0.000 03 (5)	−0.000 10 (4)
C(8)	0.0176 (4)	0.0188 (4)	0.000 372 (9)	−0.0042 (4)	−0.000 21 (5)	−0.000 01 (5)
C(9)	0.0195 (5)	0.0183 (4)	0.000 401 (10)	−0.0049 (4)	0.000 12 (6)	0.000 14 (5)
C(10)	0.0194 (4)	0.0167 (4)	0.000 323 (8)	0.0005 (4)	−0.000 06 (5)	0.000 05 (5)
C(11)	0.0196 (5)	0.0207 (4)	0.000 376 (10)	−0.0042 (4)	−0.000 04 (5)	−0.000 03 (5)
C(12)	0.0177 (4)	0.0177 (4)	0.000 404 (9)	−0.0043 (4)	−0.000 47 (6)	−0.000 24 (5)
C(13)	0.0356 (9)	0.0342 (8)	0.000 496 (13)	−0.0082 (7)	0.000 03 (9)	0.001 67 (8)
O(1)	0.0279 (4)	0.0545 (7)	0.000 503 (9)	0.0047 (4)	−0.000 63 (5)	0.001 89 (6)
O(2)	0.0161 (3)	0.0363 (5)	0.000 580 (9)	0.0021 (3)	0.000 21 (4)	0.000 27 (5)
O(3)	0.0292 (4)	0.0270 (4)	0.000 339 (7)	−0.0056 (3)	−0.000 24 (4)	0.000 62 (4)
H(2)	4.9 (0.5)					
H(3)	5.0 (0.5)					
H(6)	5.0 (0.5)					
H(8)	4.0 (0.4)					
H(9)	4.9 (0.4)					
H(11)	4.8 (0.5)					
H(12)	4.4 (0.4)					
H(13A)	6.8 (0.7)					
H(13B)	10.0 (0.9)					
H(13C)	7.1 (0.6)					

[a] Anisotropic temperature factors are expressed in the form, $\exp[-(\beta_{11}h^2 + \beta_{22}k^2 + \beta_{33}l^2 + 2\beta_{12}hk + 2\beta_{13}hl + 2\beta_{23}kl)]$. Isotropic temperature factors are expressed as $\exp[-B_\theta \sin^2\theta/\lambda^2)$. [b] Estimated standard deviations are given in parentheses.

Table III. Atomic coordinates in Fractional Crystal Coordinates for **1b**[a,b]

Atom	x	y	z
C(1)	0.5168 (2)	0.4728 (3)	0.398 64 (10)
C(2)	0.4198 (2)	0.4161 (4)	0.428 66 (11)
C(3)	0.3370 (2)	0.3615 (4)	0.398 64 (10)
C(4)	0.3380 (2)	0.3499 (3)	0.335 79 (9)
C(5)	0.4312 (2)	0.4283 (3)	0.304 58 (9)
C(6)	0.5145 (2)	0.4801 (3)	0.336 24 (10)
C(7)	0.4296 (2)	0.4433 (3)	0.242 01 (9)
C(8)	0.5232 (2)	0.4215 (3)	0.210 69 (9)
C(9)	0.5249 (2)	0.4417 (3)	0.152 70 (10)
C(10)	0.4339 (2)	0.4850 (3)	0.122 56 (9)
C(11)	0.3406 (2)	0.5083 (4)	0.152 17 (13)
C(12)	0.3400 (2)	0.4870 (3)	0.210 90 (10)
C(13)	0.3542 (2)	0.5333 (6)	0.031 43 (12)
O(1)	0.5955 (1)	0.5160 (3)	0.425 76 (7)
O(2)	0.2657 (1)	0.2723 (2)	0.311 13 (7)
O(3)	0.4455 (1)	0.5023 (3)	0.064 73 (7)
H(2)	0.424 (2)	0.432 (4)	0.472 0 (12)
H(3)	0.268 (2)	0.288 (4)	0.417 4 (10)
H(6)	0.575 (2)	0.543 (4)	0.319 3 (11)
H(8)	0.592 (2)	0.390 (4)	0.232 3 (9)
H(9)	0.589 (2)	0.424 (4)	0.132 1 (11)
H(11)	0.274 (2)	0.538 (3)	0.132 7 (9)
H(12)	0.276 (2)	0.501 (4)	0.231 7 (11)
H(13A)	0.309 (3)	0.434 (5)	0.035 5 (14)
H(13B)	0.322 (2)	0.655 (5)	0.043 0 (13)
H(13C)	0.389 (2)	0.550 (5)	−0.008 1 (16)

[a] Estimated standard deviations are given in parentheses. [b] For labeling of atoms, see Figure 4.

reflections within the 2θ range of 2–130° were measured using a moving-crystal moving-counter technique at a scan rate of 1° min^{-1}. The intensities of the three standard reflections remained practically constant (1–2% variation) throughout the period of data collection. Of the 1768 unique reflections, 1530 (87%) were considered to be observed at the 3σ level. No corrections were applied for absorption or extinction. The structure was solved by direct-methods using the LSAM approach.[16] Refinement by full-matrix, least-squares methods on positional and anisotropic thermal parameters for all nonhydrogen atoms and positional and isotropic thermal parameters for all hydrogen converged to give final values of R and R_w of 0.052 and 0.075, respectively. The final difference map provided no evidence for significant electron density not included in the model. The final values for the atomic coordinates and thermal parameters are given in Tables III and IV. The observed and calculated structure factors are available as supplementary material. In both structure determinations, reflections were weighted by a scheme written locally by Dieterich,[17] based on the equation given by Corfield, Doedens, and Ibers.[18] Atomic scattering curves for nonhydrogen atoms were from the compilation by Cromer and Mann,[19] while the scattering curve calculated by Stewart, Davidson, and Simpson[20] was used for hydrogen.

Analysis of Powder Photographs of 1a and 1b. Debye-Scherrer powder photographs were taken on a camera made by Charles Supper Co., using Ilford type G film and nickel-filtered Cu K_α (λ = 1.54178 Å) radiation. The geometrical positions to be expected from a powder pattern were calculated from unit cell data using the program DCALC written locally.[17] Good correlations were obtained between the calculated and observed d spacings. Powder photographs of samples of **1b** obtained by thermal reaction from **1a** were similar to those of **1b** prepared by crystallization.

Results and Discussion

Studies of the Rearrangement. Crystals of both the red and yellow forms of the anisylquinone were obtained from benzene–hexane, the form being determined by the recrystallization conditions. The yellow crystals on standing or heating showed a tendency which varied enormously from crystal to crystal to rearrange to the red. Some underwent the change in a few hours at room temperature; others underwent rearrangement only when heated above 100 °C. In order to obtain crystals with more uniform behavior, it was found helpful to age a batch of crystals at room temperature for 12 h to allow the more reactive ones to rearrange and to study only those

Table IV. Thermal Parameters for **1b**[a,b]

Atom	B_θ or β_{11}	β_{22}	β_{33}	β_{12}	β_{13}	β_{23}
C(1)	0.0058 (2)	0.0238 (6)	0.00166 (4)	0.0003 (2)	−0.00066 (7)	−0.0003 (1)
C(2)	0.0068 (2)	0.0351 (8)	0.00147 (5)	−0.0002 (3)	−0.00002 (7)	−0.0003 (2)
C(3)	0.0056 (2)	0.0362 (8)	0.00164 (5)	0.0000 (2)	0.00027 (7)	0.0002 (2)
C(4)	0.0043 (1)	0.0219 (5)	0.00172 (4)	0.0007 (2)	−0.00016 (6)	−0.0004 (1)
C(5)	0.0046 (1)	0.0173 (5)	0.00153 (4)	0.0011 (2)	−0.00010 (6)	−0.0004 (1)
C(6)	0.0048 (1)	0.0214 (6)	0.00166 (5)	−0.0003 (2)	−0.00012 (6)	−0.0001 (1)
C(7)	0.0041 (1)	0.0182 (5)	0.00151 (4)	−0.0001 (2)	−0.00012 (6)	−0.0004 (1)
C(8)	0.0041 (1)	0.0198 (5)	0.00174 (5)	0.0004 (2)	−0.00007 (6)	−0.0003 (1)
C(9)	0.0043 (1)	0.0223 (6)	0.00174 (5)	0.0000 (2)	0.00041 (6)	−0.0001 (1)
C(10)	0.0052 (1)	0.0212 (5)	0.00154 (5)	−0.0004 (2)	0.00021 (6)	−0.0002 (1)
C(11)	0.0045 (1)	0.0298 (7)	0.00150 (4)	0.0012 (3)	−0.00022 (6)	−0.0004 (1)
C(12)	0.0042 (1)	0.0270 (6)	0.00155 (4)	0.0012 (2)	0.00017 (6)	−0.0007 (1)
C(13)	0.0069 (2)	0.0445 (11)	0.00154 (5)	−0.0002 (4)	−0.00030 (8)	−0.0001 (1)
O(1)	0.0067 (1)	0.0400 (6)	0.00187 (3)	−0.0024 (2)	−0.00116 (6)	−0.0004 (1)
O(2)	0.0048 (1)	0.0301 (5)	0.00208 (3)	−0.0019 (2)	−0.00036 (4)	−0.0004 (1)
O(3)	0.0061 (1)	0.0377 (6)	0.00138 (3)	0.0002 (2)	0.00023 (5)	0.0004 (1)
H(2)	5.6 (0.6)					
H(3)	5.9 (0.6)					
H(6)	6.0 (0.7)					
H(8)	4.7 (0.5)					
H(9)	5.8 (0.6)					
H(11)	4.1 (0.5)					
H(12)	6.7 (0.7					
H(13A)	8.6 (1.0)					
H(13B)	8.6 (1.0)					
H(13C)	8.9 (0.9)					

[a] Anisotropic temperature factors are expressed in the form, $\exp[-(\beta_{11}h^2 + \beta_{22}k^2 + \beta_{33}l^2 + 2\beta_{12}hk + 2\beta_{13}hl + \beta_{23}kl)]$. Isotropic temperature factors expressed as $\exp[-B_\theta \sin^2\theta/\lambda^2]$. [b] Estimated standard deviations are given in parentheses.

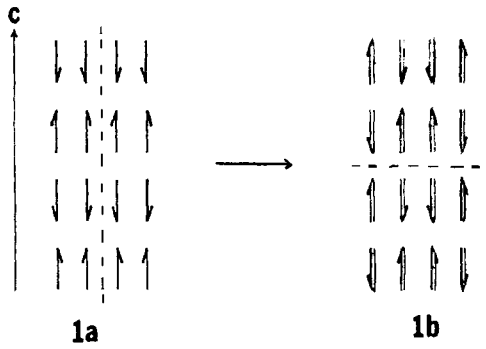

Figure 2. The arrows point in the direction of the vector from the center of the quinone ring to the anisyl ring. ↑ refers to a molecule with the chirality shown in A, ↑ to the mirror image. A similar convention applies to the molecules of **1b**, diastereomerically related to **1a**. The dotted lines outline the unit cell in each structure.

which survived this test unchanged. When the yellow compound **1a** was submitted to DSC, a small exotherm (<1 kcal/mol) was observed at about 70 °C with no sign of a melting endotherm until the melting point (121–122 °C) of the red form **1b** was reached. Examination of single crystals on a hot stage showed the behavior illustrated in the series of pictures in Figure 1. Reaction began at a region in the interior of the crystal and one or more reaction fronts developed along specific crystal directions, [110] and the symmetry-related [1$\bar{1}$0]. The reaction fronts then moved slowly through the crystal. X-ray powder photography showed that the red form obtained in this manner was identical with **1b** from recrystallization. Furthermore, a reacted "single" crystal mounted in a powder camera without grinding gave a satisfactory powder photograph but with some arc-like streaks, indicating a small amount of net orientation of the product. These general features of the reaction are highly reminiscent of the solid state change of the

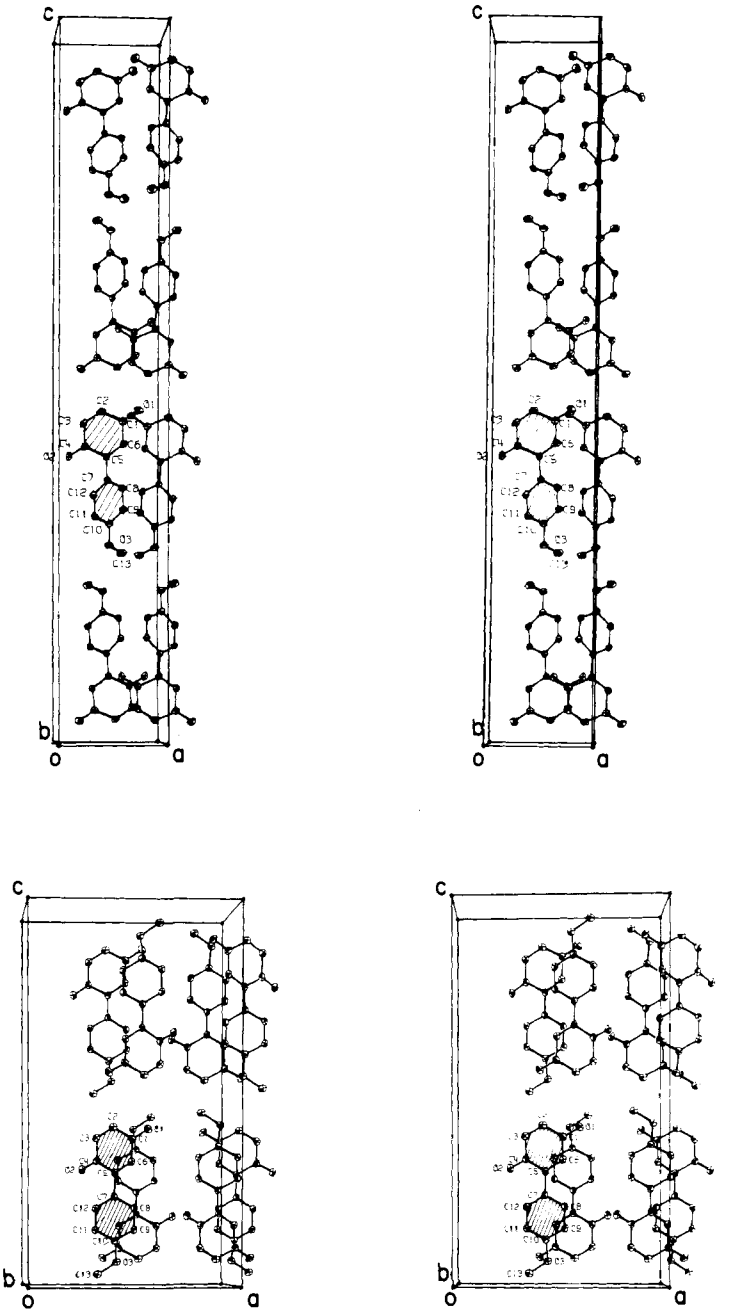

Figure 3. The upper stereopair shows the yellow form (**1a**) of 2-(4′-methoxyphenyl)-1,4-benzoquinone; the lower stereopair shows the red form (**1b**). The shaded molecules are those whose parameters are given in Tables I–IV.

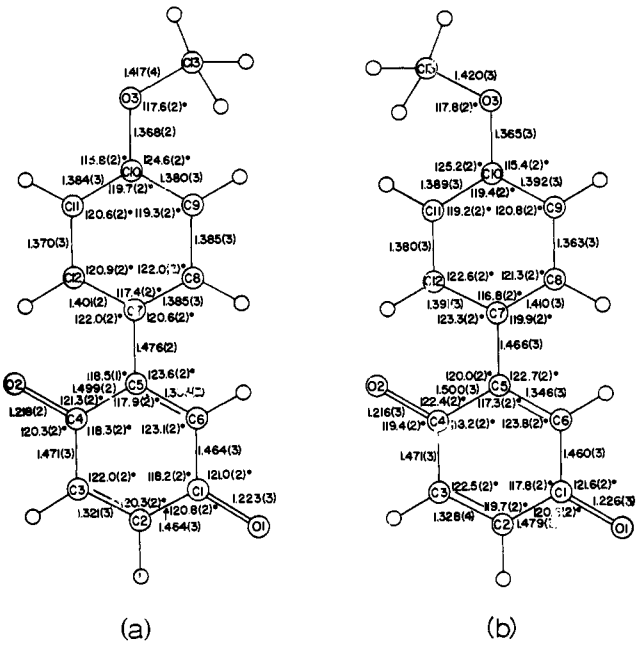

Figure 4. Left: bond lengths and angles involving nonhydrogen atoms for **1a**. Right: the same for **1b**.

yellow (**2a**) to the white form (**2b**) of the hydroxyterephthalate ester[11] in spite of the great difference in the structures and in the nature of the change involved in the two systems.

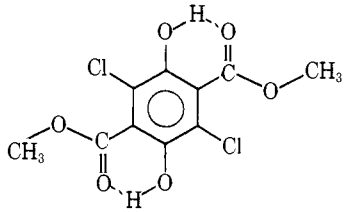

2a

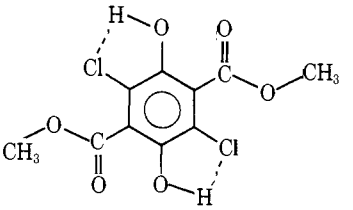

2b

Structural Change. The crystal structures of the anisylquinones showing the nature of the change from **1a** to **1b** are illustrated in Figures 2 and 3. Bond lengths and angles in **1a** and **1b** are shown in Figures 4a and 4b.

In both forms, the six carbon atoms of the anisyl ring approach coplanarity, while the atoms of the quinone ring are significantly nonplanar. In **1a,** the distance of the carbon atoms from the best plane through the six atoms of the quinone ring range from −0.035 to 0.023 Å with O(1) and O(2) lying −0.006 and −0.172 Å from that plane; in **1b,** the corresponding distances are −0.037 to 0.055 with O(1) and O(2) lying 0.105 to 0.243 Å from the plane. This "bowing" effect has been reported for some other quinones[21] especially halogenated quinones. The angles between the best planes through the two rings are 38.9 and 31.9° in **1a** and **1b,** respectively. The required minimal change in molecular structure can be seen by comparison of the two shaded molecules in Figure 3 to involve a partial rotation of the anisyl ring together with its nearly coplanar methoxyl group from the conformation A with a

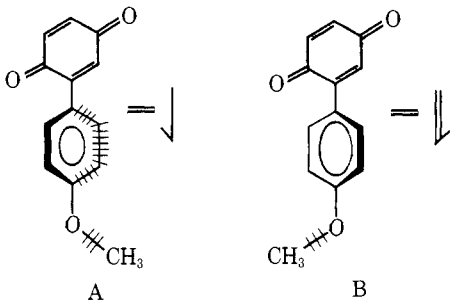

A B

ring–ring angle of 39° to B with a ring–ring angle of 32°. Such a rotation were it to occur in solution would have little or no energy barrier, but, of course, the crystal structure of A locks the rings in such a way that extensive reorganization is required for such a change of molecular shape. Molecules A and B are each chiral and are diastereomeric. By virtue of crystallization in the space group *Pbca*, each is accompanied necessarily by its mirror image in its respective structure.

Further analysis of the structural change in Figure 3 shows that in each crystal structure the long molecular axis is roughly parallel to *c*. Although the space group is the same in each case, the isomer **1a** has the quinone molecules distributed so as to form a structure with four layers of molecules along *c* such that all anisylquinone molecules are arranged in a "head-to-head" fashion with the quinone portions of the molecules adjacent to quinone rings and the anisyl groups to anisyl groups. The red isomer **1b,** however, is a structure with two layers along *c*; each layer contains four molecules arranged in pairs "head-to-tail". If molecules A and B are designated by the types of arrows shown beside the structures, the packing of the crystal can be represented for two unit cells as in Figure 2.[22] Clearly a transformation of **1a** to **1b** requires that either, by slippage along *c*, molecules in adjacent layers become mixed, or that molecules reorient their direction along *c* a full 180° around an axis perpendicular to their long direction.

Although we have no knowledge of the degree of disorder of states intermediate in the rearrangement of **1a** to **1b,** it is of interest to analyze the two structures with the aim of finding a path of minimal disorder. In Figure 1 it is shown that the transformation proceeds by formation or reaction fronts lying in the [110] and [1$\bar{1}$0] directions. This observation focuses attention on the (1$\bar{1}$0) and (110) planes which contain the [110] and [1$\bar{1}$0] vectors. In Figure 5 are stereopair drawings of **1a** and **1b,** the drawing of **1a** having a selection of molecules chosen to bring out the structure of a layer parallel to (1$\bar{1}$0) and the structure of **1b** showing a corresponding layer parallel to (2$\bar{1}$0) (the *a* axis is approximately doubled in structure **1b**). Careful examination of these drawings shows that it is possible to derive structure **1b** from **1a** by shifting molecules in the layer indicated and with no rotation more severe that the minimum anisyl ring rotation which is required to go from the enantiomeric conformers of **1a** to their diastereomers constituting **1b.** Such a "slip mechanism" causing rapid rearrangement through the interior of each successive layer of molecules parallel to (110) or (1$\bar{1}$0) explains the observed formation of fronts parallel to [1$\bar{1}$0] and [110] vectors and is reminiscent of the recent proposal of Parkinson, Thomas, Williams, Goringe, and Hobbs[23] that the phase transition interconverting α- and β-5-methyl-1-thia-5-aza-cyclooctane-1-oxide perchlorate[24] occurs by the recurrent passage of glissile partial dislocations on contiguous planes. It is of interest in this connection that the rearrangement of **1a** to **1b** is initiated at a surface formed by fracture of a crystal where slip dislocations are likely to have been introduced.[25] It should be stated, however, that we have no direct evidence bearing on the question of the extent of disorder occurring during the rearrangement. Clearly, as indicated by the formation of a rea-

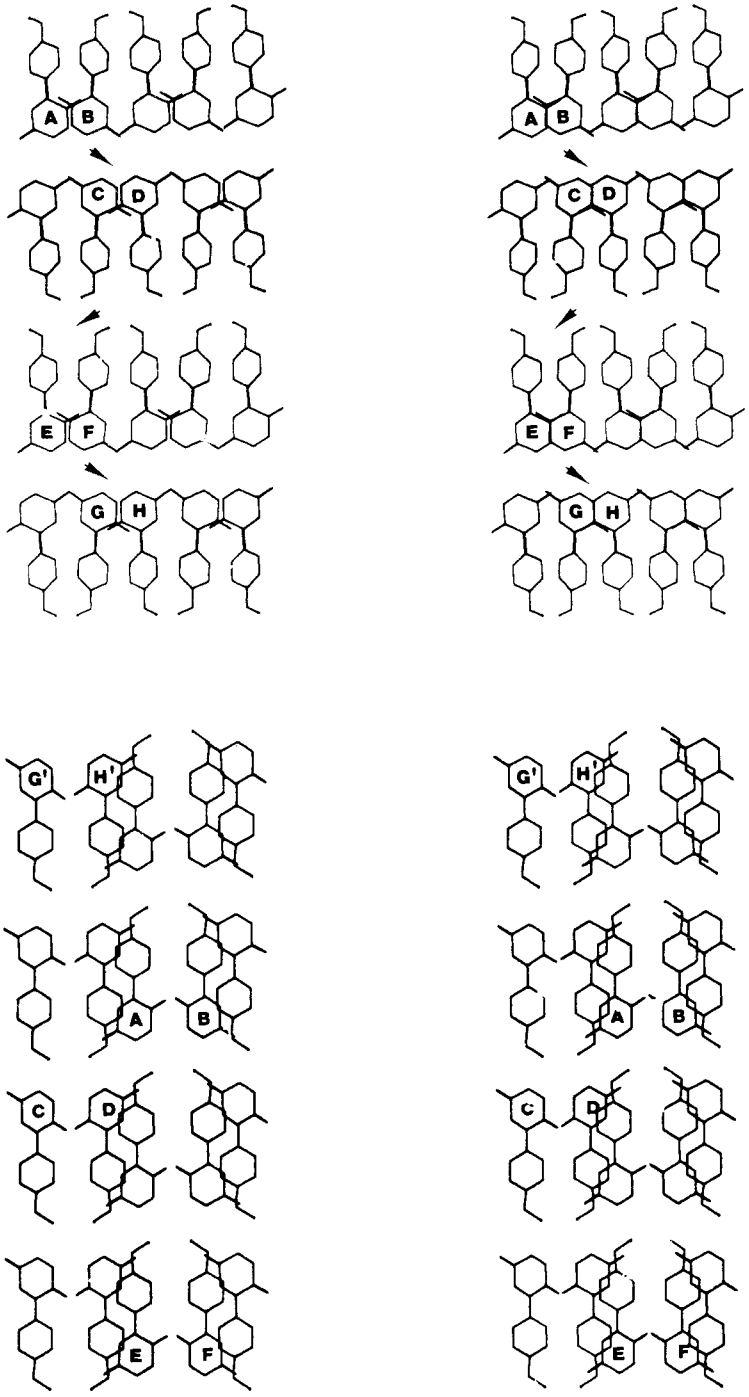

Figure 5. Stereopairs of **1a** (upper) and **1b** (lower) oriented as in Figure 3 but with a selection of molecules forming the $(1\bar{1}0)$ plane of **1a** and a corresponding set of **1b.** The transition from **1a** to **1b** can be formulated as involving the slide of the lettered molecules from one layer to the next as indicated by the arrows. The molecules which have undergone such translation are lettered correspondingly in the lower drawing.

sonable powder photograph from an unground crystal after completion of reaction the product has reorganized itself into microcrystallites whose average dimension is hundreds to thousands of molecules in length. This kind of reorganization of a reacting solid has been observed in many other examples.[3]

It may be noted that Mnyukh, Panfilova, Petropavlov, and Uchvatova[26] in an analysis of a number of phase transitions have suggested that rearrangement occurs at a series of microcavities at the reactant-product interface, when as here the orientations of reactant and product lattices are not correlated. They concluded that, "There is no indication that a polymorphic transition can be achieved by a "shift", a "turn", a "displacement", an "expansion", a "deformation", or an "overturn" of the original crystal structure to the final one". Clearly, more experimental evidence is needed before we can draw further conclusions about the detailed mechanism of the transformation of **1a** to **1b.**[27]

Molecular Stacking in the Yellow (1a) and Red (1b) Forms of 2-(4'-Methoxyphenyl)-1,4-benzoquinone. The difference in color of **1a** and **1b** had attracted earlier attention and a comparison[8] of the uv-visible spectra of the solids compared with the melt and solution had led to the suggestion that the red color of **1b** was due to charge-transfer interaction of the anisyl ring of one molecule with the quinone ring of its neighbor. The x-ray crystal structure of **1b** reported here confirms this proposal and has features which merit further discussion. The overlap between a pair of rings is illustrated in Figure 6 and

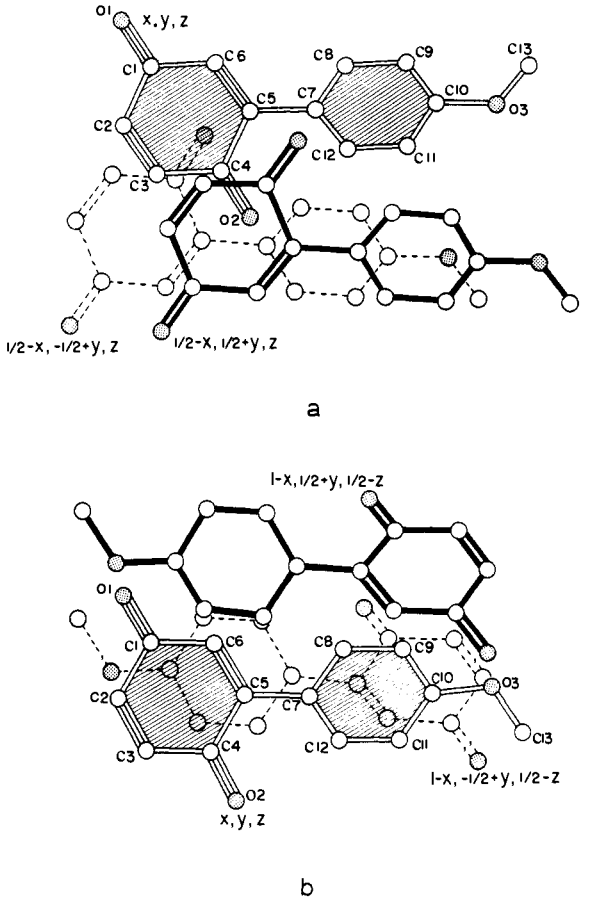

Figure 6. Projections showing the overlap of molecules (a) for **1a** and (b) for **1b.** In each drawing the atoms are projected onto the best plane through the quinone ring in the central (line shaded) molecule. The molecules with dark bonds lie above the reference plane, those with dashed lines are below.

is rather typical of the geometrical arrangement of other π complexes.[21] The anisyl ring in the molecule at $1 - x, -\frac{1}{2} + y, \frac{1}{2} - z$ overlaps the quinone ring (C(1)-C(6)) in the reference molecule; the least-squares planes of these rings are inclined at an angle of 11°. The overlap pattern leads to distances between C(1), C(1), C(2), and C(4) in the reference molecule and C(10), O(3), O(3), and C(9) in the molecule at $1 - x, -\frac{1}{2} + y, \frac{1}{2} - z$ of 3.49, 3.42, 3.36, and 3.35 Å, respectively. These distances indicate a moderately strong charge-transfer interaction. There are contacts of 3.27 and 3.30 Å between C(9) and C(8) in the reference molecule and C(6) in the molecule at $1 - x, -\frac{1}{2} + y, \frac{1}{2} - z$, but, due to the tilt of the rings, there is no overlap between the anisyl group in the reference molecule and the quinone ring in the molecule at $1 - x, -\frac{1}{2} + y, \frac{1}{2} - z$. An interesting aspect of the stacking arrangement is that the quinone ring of a molecule of **1b** overlaps with only one adjacent anisyl group but on the other end the anisyl group of the first molecule overlaps with a quinone ring of a third molecule. There is thus a continuous chain held together by π complexing but each ring has only one close neighbor. This is illustrated in Figure 7. Other examples of self-complexing molecules have been reported recently.[28-30]

The yellow structure **1a** is also of interest. In this case, there is no possibility for quinone–anisyl ring overlap and instead the point of interest is the overlap between adjacent quinone rings which is also shown in Figure 6. Although this type of overlap is not found in the packing of most quinones, it is of interest that it is very similar to that of a quinone-like spirodienone **4.**[31]

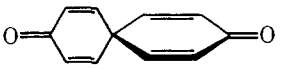

4

The π complexing possible in **1b** but not in **1a** must contribute to the determination of the position of the equilibrium between them. However, it should be noted that the yellow form of the *o*-methoxy isomers of **1a** and **1b** is the more stable, in spite of the apparent lack of π complexing.

A comparison of the bond distances (Figure 4) in the yellow and red forms of **1** is interesting in view of the difference in stacking in the two structures. Although the differences are

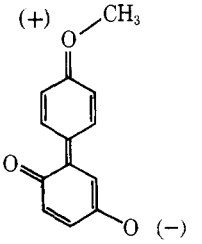

C

small, they are in the direction to be expected if the π overlap of anisyl with quinone rings found in **1b** served to increase the contribution of the dipolar resonance structure C to the structure of **1b.**

Acknowledgment. We wish to thank Mr. Al Saldeen for assistance in preparing photographs for publication. Mrs. Patti Eckert and Miss Mary K. Greensley contributed to the drafting of the paper.

Supplementary Material Available: A listing of structure factor amplitudes, some details of best planes, and short intermolecular contacts (27 pages). Ordering information is given on any current masthead page.

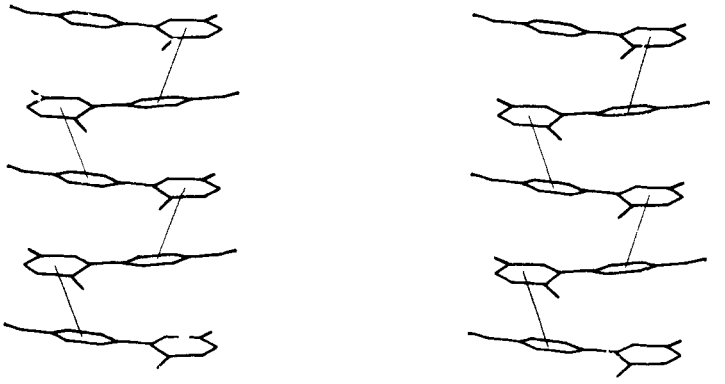

Figure 7. Stereopair drawing of a stack of molecules of **1b** showing the quinone–anisyl interaction. The molecules are stacked along the vertical (*b*) axis.

References and Notes

(1) Taken from the Ph.D. Thesis of Gautam R. Desiraju, submitted to the University of Illinois, 1976, available from University Microfilms, Ann Arbor, Mich.
(2) We are indebted to the National Science Foundation (NSF DMR 7203026) for support of this work.
(3) I. C. Paul and D. Y. Curtin, *Acc. Chem. Res.*, **6**, 217 (1973); *Science*, **187**, 19 (1975).
(4) M. D. Cohen and B. S. Green, *Chem. Brit.*, **9**, 490 (1973).
(5) J. M. Thomas, *Philos. Trans. R. Soc. London*, **277**, 251 (1974).
(6) D. E. Kvalnes, *J. Am. Chem. Soc.*, **56**, 2478 (1934).
(7) M. Akagi and K. Hirose, *Yakhak Hoe Chi*, **62**, 191 (1942).
(8) J. Aihara, G. Kushibiki, and Y. Matsunaga, *Bull. Chem. Soc. Jpn.*, **46**, 3584 (1973); J. Aihara, *ibid.*, **47**, 2063 (1974).
(9) P. Brassard and P. L'Ecuyer, *Can. J. Chem.*, **36**, 700 (1958).
(10) While no quantitative work was carried out, estimates based on peak areas suggested a ΔH for the exotherm of ≤ 1 kcal/mol, a value comparable with those for similar transitions in organic solids.[11]
(11) S. R. Byrn, D. Y. Curtin, and I. C. Paul, *J. Am. Chem. Soc.*, **94**, 890 (1972).
(12) We observed some reflections in the *hk*0 net that we considered might be indicative of a different space group. However, upon further examination we believe that these are either Reninger reflections from strong *h*00 reflections or are really *hkl* reflections that had not been completely excluded by the layer line screen on the precession camera ($c = 44.206$ Å).
(13) R. S. Miller, I. C. Paul, and D. Y. Curtin, *J. Am. Chem. Soc.*, **96**, 6334 (1974).
(14) R. B. K. Dewar, Ph.D. Thesis, University of Chicago, 1968.
(15) $R = \Sigma|(F_{obsd}) - (F_{calcd})|/\Sigma(F_{obsd})$; $R_w = [\Sigma w|(F_{obsd}) - (F_{calcd})|^2/\Sigma w(F_{obsd})^2]^{1/2}$.
(16) This program was written by P. Main and M. M. Woolfson, University of York, York, England (1972).
(17) D. A. Dieterich, Ph.D. Thesis, University of Illinois, Urbana, 1973.
(18) P. W. R. Corfield, R. J. Doedens, and J. A. Ibers, *Inorg. Chem.*, **6**, 197 (1967).
(19) D. T. Cromer and J. B. Mann, *Acta Crystallogr., Sect. A*, **24**, 321 (1968).
(20) R. F. Stewart, E. R. Davidson, and W. T. Simpson, *J. Chem. Phys.*, **42**, 3175 (1965).
(21) J. Bernstein, M. D. Cohen, and L. Leiserowitz in "The Chemistry of Quinonoid Compounds", Part 1, S. Patai, Ed., Wiley, London, 1976, Chapter 2.
(22) The reason that the same symmetry operations produce a four-rowed structure for **1a** and a two-rowed structure for **1b** follows immediately from the observation that the center of the parent molecule in **1a** has a value of $z \approx 1/8$ while **1b** has a $z \approx 1/4$. Since the space group in each case has molecules at z, $1/2 - z$, $1/2 + z$, and $-z$ (two molecules with each z-value) it follows that **1a** has two molecules each at $z = 1/8, 3/8, 5/8$, and $7/8$ while **1b** has four molecules at $z = 1/4$ and four at $z = 3/4$.
(23) G. M. Parkinson, J. M. Thomas, J. O. Williams, M. J. Goringe, and Linn W. Hobbs, *J. Chem. Soc., Perkin Trans. 2*, 836 (1976).
(24) I. C. Paul and K. T. Go, *J. Chem. Soc. B*, 33, (1969).
(25) A more detailed analysis of this and other mechanistic possibilities is given in ref 1.
(26) Yu. V. Mnyukh, N. A. Panfilova, N. N. Petropavlov, and N. S. Uchvatova, *J. Phys. Chem. Solids*, **36**, 127 (1975); Yu. V. Mnyukh and N. A. Panfilova, *ibid.*, **34**, 159 (1973).
(27) Since the completion of this work, we became aware of a report of dimorphism of a complex quinone with some features similar to those observed here. [C. H. Girffiths, M. S. Walker, P. Goldstein, and R. L. Miller, *Mol. Cryst. Liq. Cryst.*, **31**, 295 (1975)].
(28) A. E. Shvets, Ya. Ya. Bleidelis, and Ya. F. Freimanis, *Zh. Strukt. Khim.*, **16**, 640 (1975), and earlier references there cited.
(29) R. Carruthers, F. M. Dean, L. E. Houghton, and A. Ledwith, *Chem. Commun.*, 1206 (1967).
(30) C. K. Prout and E. Castellano, *J. Chem. Soc. A.*, 2775 (1970).
(31) D. L. Cullen, B. Haas, D. G. Klunk, T. V. Willoughby, C. N. Morimoto, E. F. Meyer, Jr., G. Farges, and A. Dreiding, *Acta Crystallogr., Sect. B*, **32** 555 (1976).

Kinetic Isotope Effect on Proton Tautomerism in Tetraarylporphyrins

S. S. Eaton*[1a] and G. R. Eaton*[1b]

Contribution from the Department of Chemistry, University of Colorado at Denver, Denver, Colorado 80202, and the Department of Chemistry, University of Denver, Denver, Colorado 80210.

Received August 3, 1976

Abstract: Rates and activation parameters for proton and deuteron tautomerism in tetrakis(pentafluorophenyl)porphyrin, tetrakis(*p*-trifluoromethylphenyl)porphyrin, tetrakis(*p*-isopropylphenyl)porphyrin, and tetrakis(*p*-diethylaminophenyl)porphyrin have been obtained by variable-temperature proton NMR and total line shape analysis. Rates are independent of concentration, phenyl ring substituents, and solvent, consistent with a mechanism involving simultaneous movement of the two hydrogens through a symmetrical transition state. Based on six independent sets of data, the ratio of the rates for proton and deuteron tautomerism, k_H/k_D, at 298, 263, and 243 K is 19 ± 5, 32 ± 7, and 48 ± 14, respectively. The large values of k_H/k_D are attributed to simultaneous exchange of the two hydrogens.

Proton tautomerism in porphyrins was first demonstrated by Storm and Teklu using variable-temperature ^{1}H NMR.[2a] At slow exchange two pyrrole β-proton resonances were observed and were assigned to pyrrole rings with and without a proton on the pyrrole nitrogen. Tautomerism (I $\rightleftharpoons$ II) averages

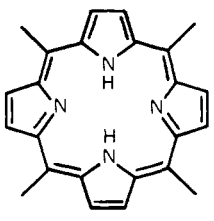

I

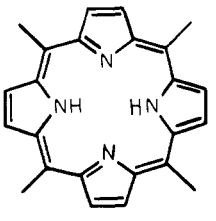

II

the two environments. The isotope effect on the rate of tautomerism, k_H/k_D, was first estimated to be 67 for tetraphenylporphyrin,[2b] but later a value of 12 was obtained by comparison of rates estimated from ^{1}H and ^{13}C NMR spectra at 35 °C.[3] Because of the widespread interest in porphyrins it appeared worthwhile to obtain more accurate estimates of the kinetic isotope effect by performing a total line shape analysis of the spectra over the full exchange region. It was also of interest to determine whether the isotope effect on proton tautomerism in porphyrins is a case in which the isotope effect relates to the exactly equivalent motion of two hydrogens.

Recent papers have shown that phenyl ring substituents in tetraarylporphyrins influence rates of copper ion incorporation,[4] equilibrium constants for piperidine binding to Ni^{2+}, Co^{2+}, and $(VO)^{2+}$ porphyrins,[5,6] equilibrium constants for pyridine coordination to Zn^{2+} and Co^{2+} porphyrins,[6,7] basicity of free porphyrins,[8] electronic spectra of free porphyrins,[8] and redox potentials of Ni^{2+} and Co^{2+} porphyrins and free porphyrins[6,9,10] in accordance with Hammett correlations. It was therefore of interest to determine whether similar effects would be observed for proton tautomerism.